Formation of the double stratopause and elevated stratopause associated with the major stratospheric sudden warming in 2018/19

Haruka Okui[1], Kaoru Sato[1], Dai Koshin[1], and Shingo Watanabe[2]

[1]Department of Earth and Planetary Science, The University of Tokyo, Tokyo, Japan
[2]Japan Agency for Marine–Earth Science and Technology, Yokohama, Japan

Stratopause during a sudden stratospheric warming

Variation of the stratopause during a sudden stratospheric warming (SSW)

(1) -Day 0 (SSW onset) :
Stratopause descent (z=~55km→30km)
(2) Day ~+5 : Disappearance
(3) Day ~+10 : Reformation at z=~80km
= **Elevated stratopause (ES)**

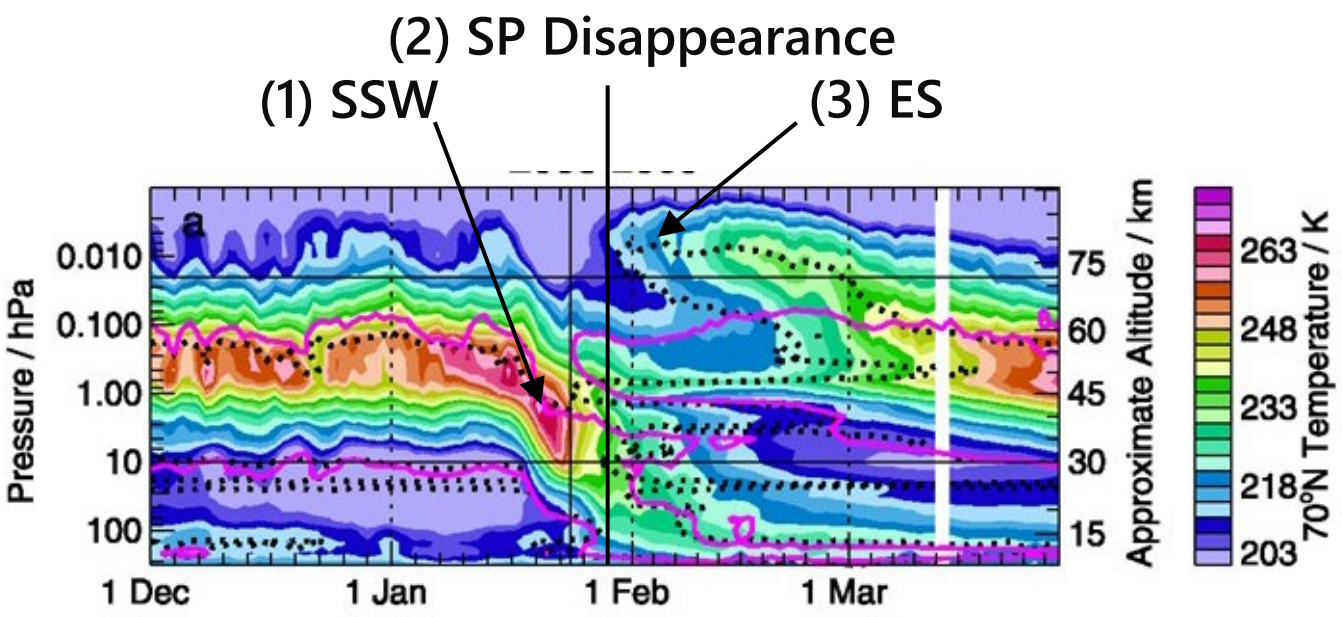

70°N time-pressure section of zonal mean temperature from the Aura Microwave Limb Sounder (MLS) during the 2009 SSW event. Adapted from Manney et al. [2009].

Possible mechanisms of the ES formation:

- Gravity-wave (GW) driven [e.g., Tomikawa et al. 2012; Siskind et al. 2007, 2010]
- (At least initially) Planetary-wave (PW) driven [e.g., Limpasuvan et al. 2012, 2016]

Difficulty in ES modeling:

- Faster descent at lower altitude than observed ES events
- Underestimation of downwelling in the upper mesosphere

← Difficulty in realistic GW representation in models [e.g., Meraner et al. 2016]

To elucidate the mechanisms of ES and other MLT responses to SSWs, quantitative analysis of roles of waves including GWs is needed.

Model & simulation details

In the present study:

- A hindcast of 2018/19 SSW was carried out by a **GW-permitting** high-top general circulation model: **Japanese Atmospheric General circulation model for Upper Atmosphere Research (JAGUAR)** [Watanabe and Miyahara, 2009].
- The outputs were analyzed quantitatively and three-dimensionally.

The 2018/19 major SSW event:

- A mixed type (displacement to split) SSW
- The onset of the major warming on 1 January 2019

Model & simulation details:

Vertical domain	~ 0–**150** km
Resolution	Horizontal res.: T639 ($\lambda_h \gtrsim$60km), Vertical res.: 300m (340 layers)
GW parameterization	**Not be used**
Initial values	Analysis data carried out by JAGUAR-T42L124 ◀ Assimilating the data from PREPBUFR, MLS, SABER and SSMIS by the **JAGUAR-DAS** system [Koshin et al. 2020, 2021]
Cycle of each simulation	1-day nudging, 2-day spin-up and **4-day free-run** ◀ **Analyzed**
Simulated period	5 December 2018 – 17 January 2019 (4-day free-run x11)

Variation in the zonal mean fields

Zonal mean zonal wind ($\bar{u}$) in 50°N-70°N:

- Westward wind ($\bar{u}$<0) forms around 25 Dec. and gradually descends to z=~30km.
- Strong eastward wind ($\bar{u}$>0) reforms at z=~65km around 10 Jan.

Zonal mean temperature ($\bar{T}$) in 70°N-80°N:

- The stratopause descends from z=~55km to ~40km associated with the SSW.
- A peak with a mesospheric inversion layer (MIL) appears at z=85-90km on 28 Dec.

→ Two $\bar{T}$ maxima in the vertical (with the stratopause)

→ Referred to as "**double stratopause (DS)**"

- The **ES** appears at z=~80km on 10 Jan.

Comparison with MERRA-2/Aura MLS/SABER:

- Mostly consistent in the stratosphere & mesosphere
- DS & ES are also observed in the MLS & SABER data

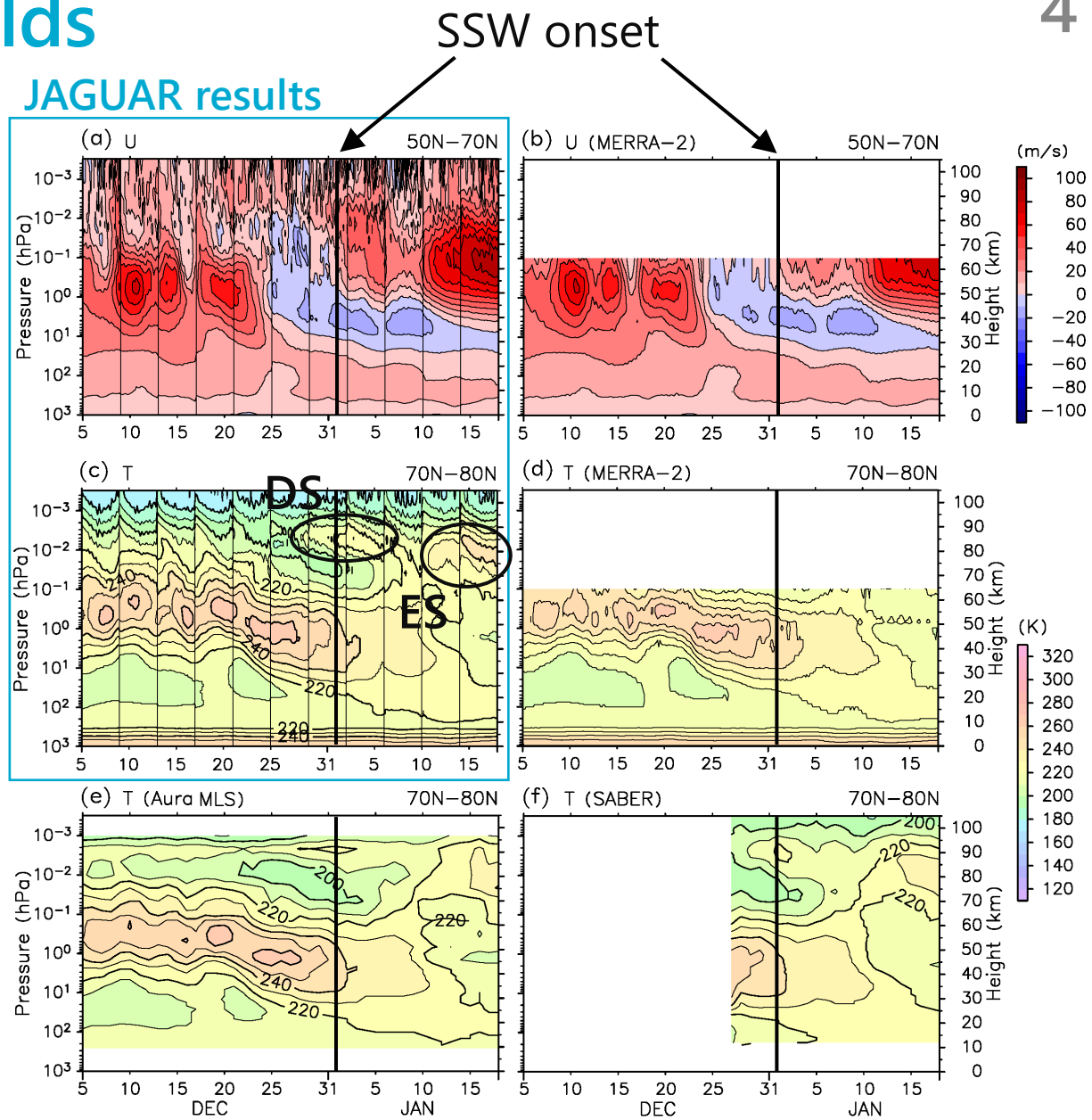

Time-height sections of 50°N-70°N mean $\bar{u}$ from (a) JAGUAR and (b) MERRA-2, and 70°N-80°N mean $\bar{T}$ from (c) JAGUAR, (d) MERRA-2, (e) Aura MLS and (f) SABER. Vertical lines in (a) and (c) represent the boundaries of the model runs.

Variation of the wave forcing

Eliassen-Palm flux divergence (EPFD) of all wave components/PWs/GWs in 50°N-70°N:

EPFD indicates wave forcing. Positive (negative) EPFD represents eastward (westward) momentum deposition.

PWs: zonal wavenumber s=1-3
GWs: total horizontal wavenumber n=21-639

When the DS forms:

- Strong negative (westward) PW forcing (PWF) at z>85km, which induces residual downward flow ($\overline{w}^*$<0) in the polar region

→ PWF contributes to the DS formation

When the ES forms:

- Strong negative PWF at z>80km
- Strong negative GW forcing (GWF) at z>70km

→ Both PWF & GWF contribute to the ES formation

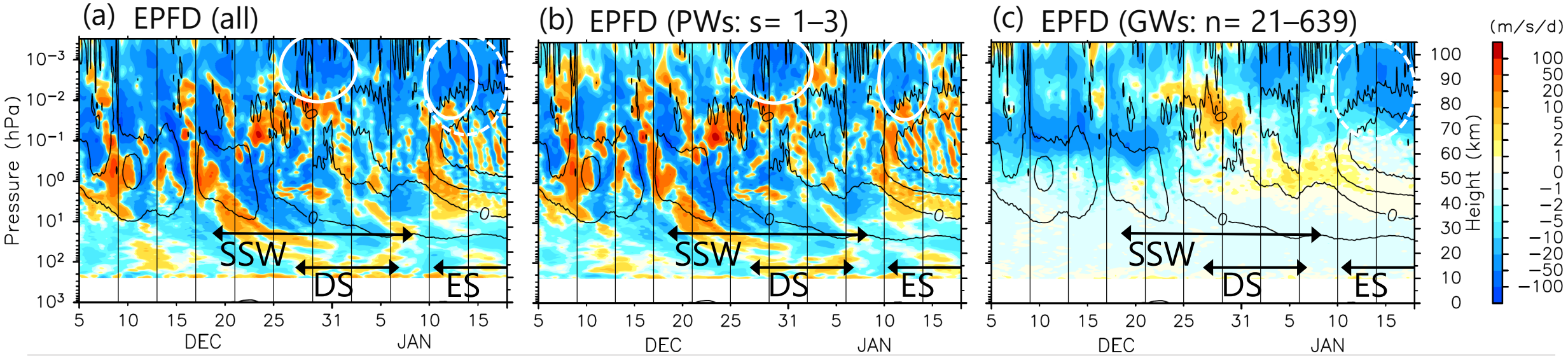

Time-height sections of 50°N-70°N mean EPFD due to (a) all wave components, (b) PWs and (c) GWs along with $\overline{u}$ (contours; interval: 20m/s). EPFD due to other components beside PWs and GWs were always small at any height or time. Vertical lines represent the boundaries of the model runs.

Longitudinal structure of the DS

The DS is observed
inside the polar vortex.

★ : The DS is clearly observed

☆ : The DS is **not** clearly observed

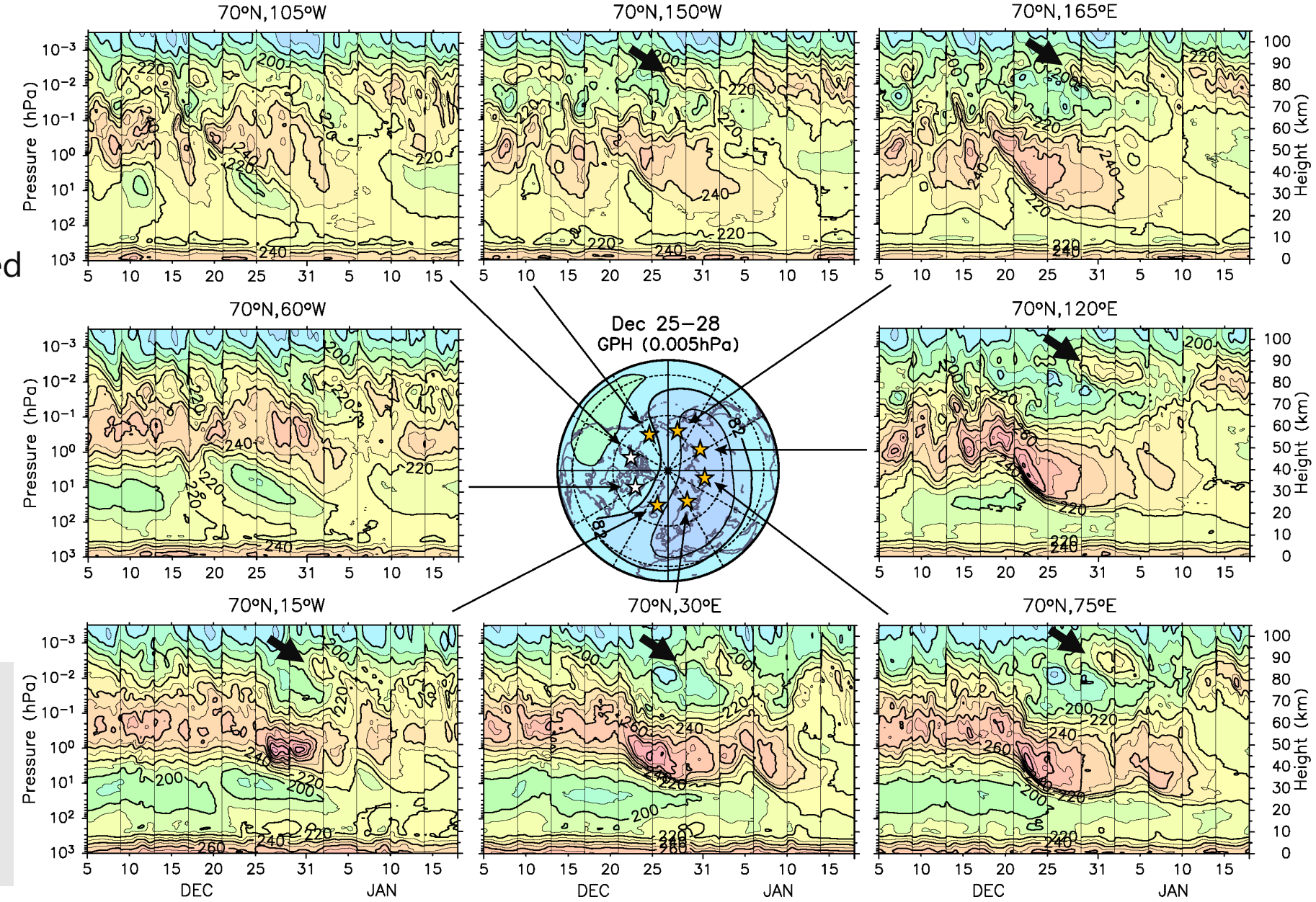

Map of GPH (unit: km) at 0.005hPa from 25-28 Dec. and time-height sections of T at each location along 70°N. The colors of stars represent the DS occurrence (yellow→the DS occurs).

Longitudinal structure of the DS

The DS is observed in the east of 120°E to 0°.

In the region with $\bar{u}$<0 at z=40-80km, upward propagation of PW is strongly attenuated. A large part of PWs from the troposphere cannot reach above z=85km.

Strong GWF>0 possibly contributes to forming the cold region at z=70-85km.

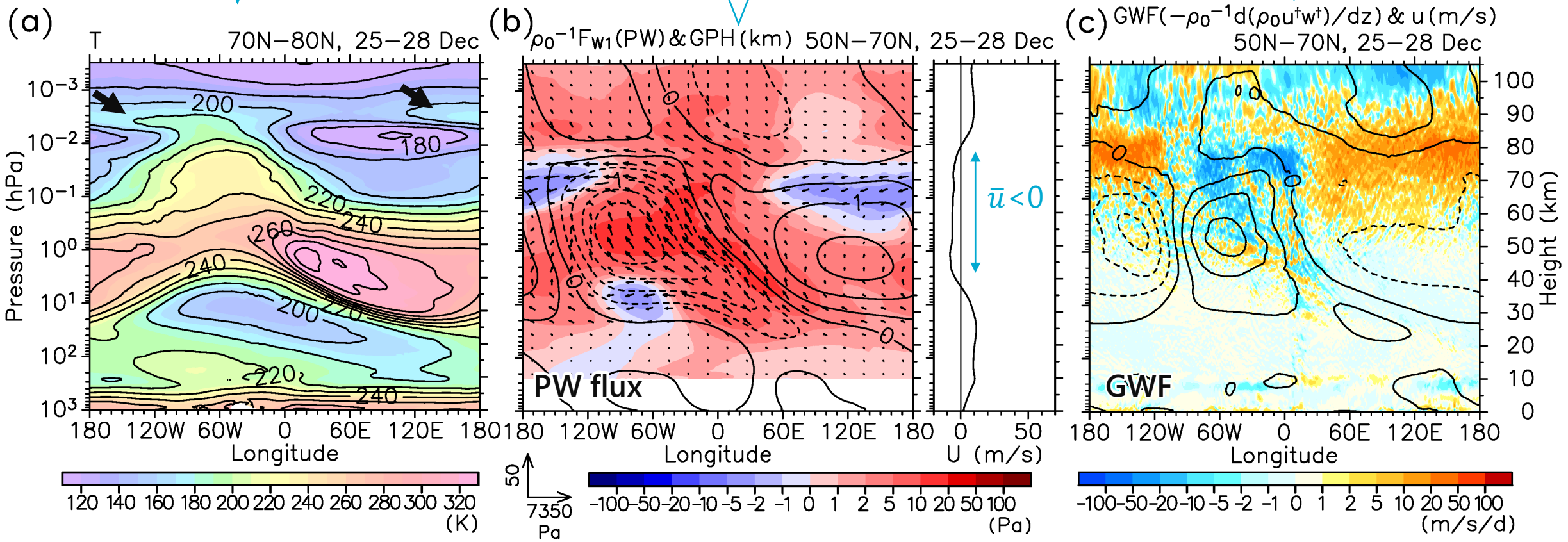

Longitude-height sections for 25-28 Dec. of (a) 50°N-70°N mean T, (b) 50°N-70°N mean 3D wave activity flux F_{W1} [Kinoshita & Sato 2013; Sato et al. 2013] (color represents the vertical component of F_{W1}) and geopotential height deviation from the zonal mean (contours; interval: 0.5km), and (c) GWF indicated by $-\rho_0^{-1}d(\rho_0 u'w')/dz$ and zonal wind u (contours; interval: 10m/s). A small box in (b) shows $\bar{u}$ profile.

DS formation: PW generation due to GWF

Modified PV (MPV) [Lait 1994]:
$\mathrm{MPV} = \mathrm{EPV} \cdot (\theta/\theta_{\mathrm{R}})^{-9/2}$
$\propto (f + \xi) \cdot N^2$

Where are PWs at z>85km from, which cause the DS formation?

(1) During 17-20 Dec., **GWF>(<)0** appears at z=~65km equatorward (poleward) of ~40°N (◯ in Fig.1d).

(2) GW-induced residual mean upward flow $\bar{w}^*>0$ converges at z=~65km(~3500K), ~40°N (↑ in Fig.1d).

(3) **Modified PV (MPV)** [Lait 1994] **peak** appears due to increase in static stability N^2 (◯ in Fig.1b & Fig.2).

(4) The necessary condition for BT/BC instability ($\overline{\mathrm{MPV}}_y<0$) is fulfilled poleward of the peak.

(5) During 21-24 Dec., **PWF>0**, which indicates PW generation, is observed poleward of the MPV peak & negative $\overline{\mathrm{MPV}}_y$ becomes small (◌ in Figs.1f & 1g).

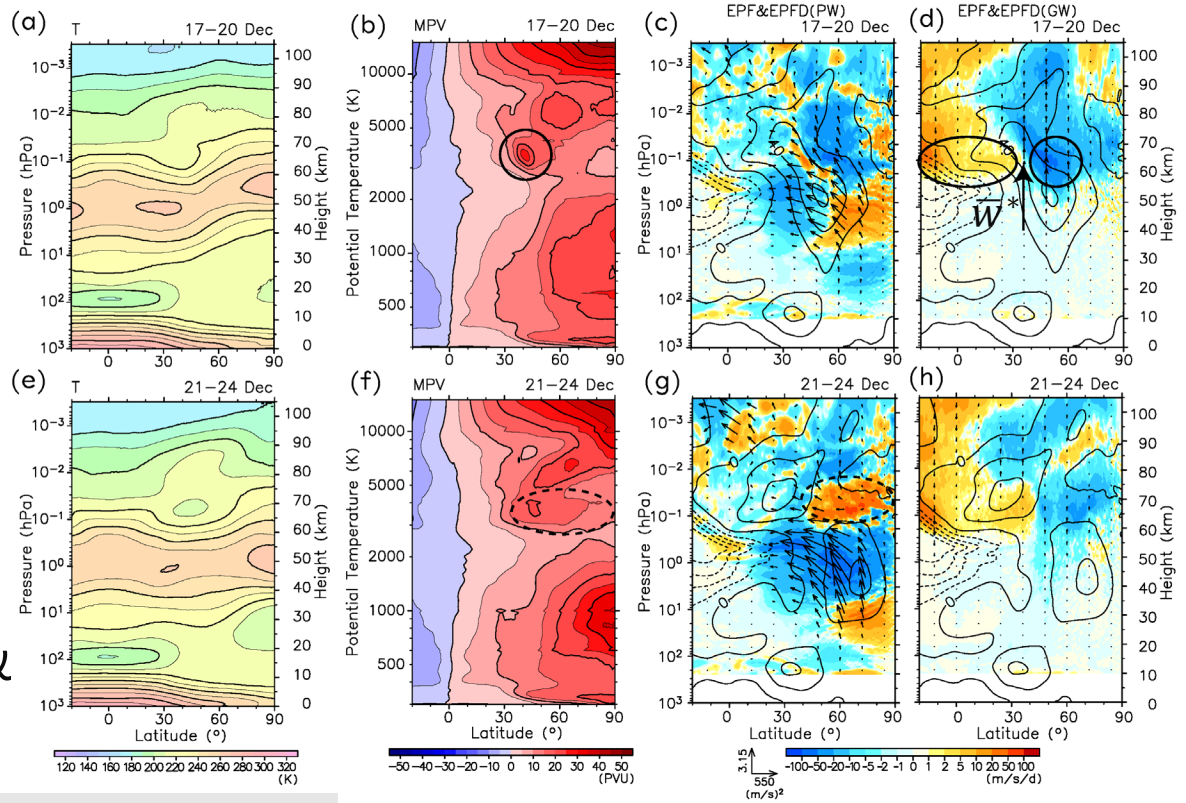

PWs are generated by the BT/BC instability which is induced by **GWF**.

PW-driven DS formation

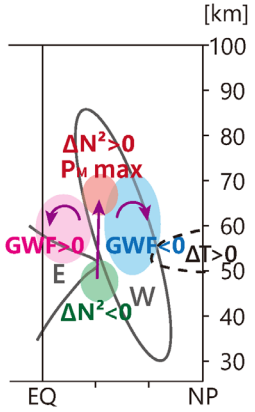

Figure 1(↗) Latitude-height sections of (a,e) $\bar{T}$, (b,f) $\overline{\mathrm{MPV}}$, (c,g) PWF and (d,h) GWF along with zonal wind u (contours; interval: 20m/s) for (a-d) 17-20 and (e-h) 21-24 Dec.

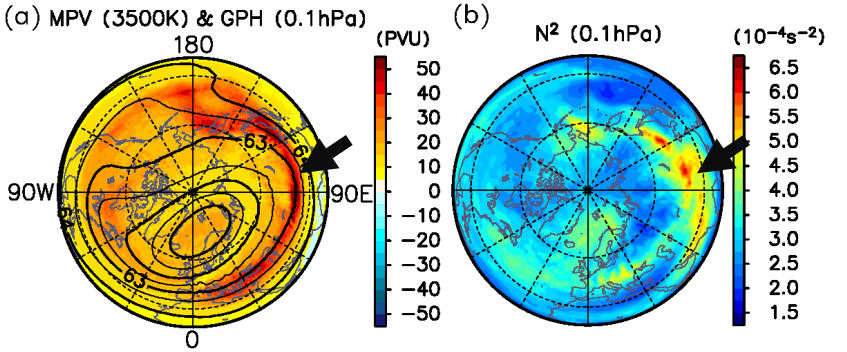

Figure 2(→) Maps at 0.1hPa for 17-20 Dec. of (a) MPV (color) and GPH (contour, unit: km) and (b) N^2

Longitudinal structure of the ES

The ES is observed
inside the polar vortex.

★ : The ES is clearly observed

☆ : The ES is **not** clearly observed

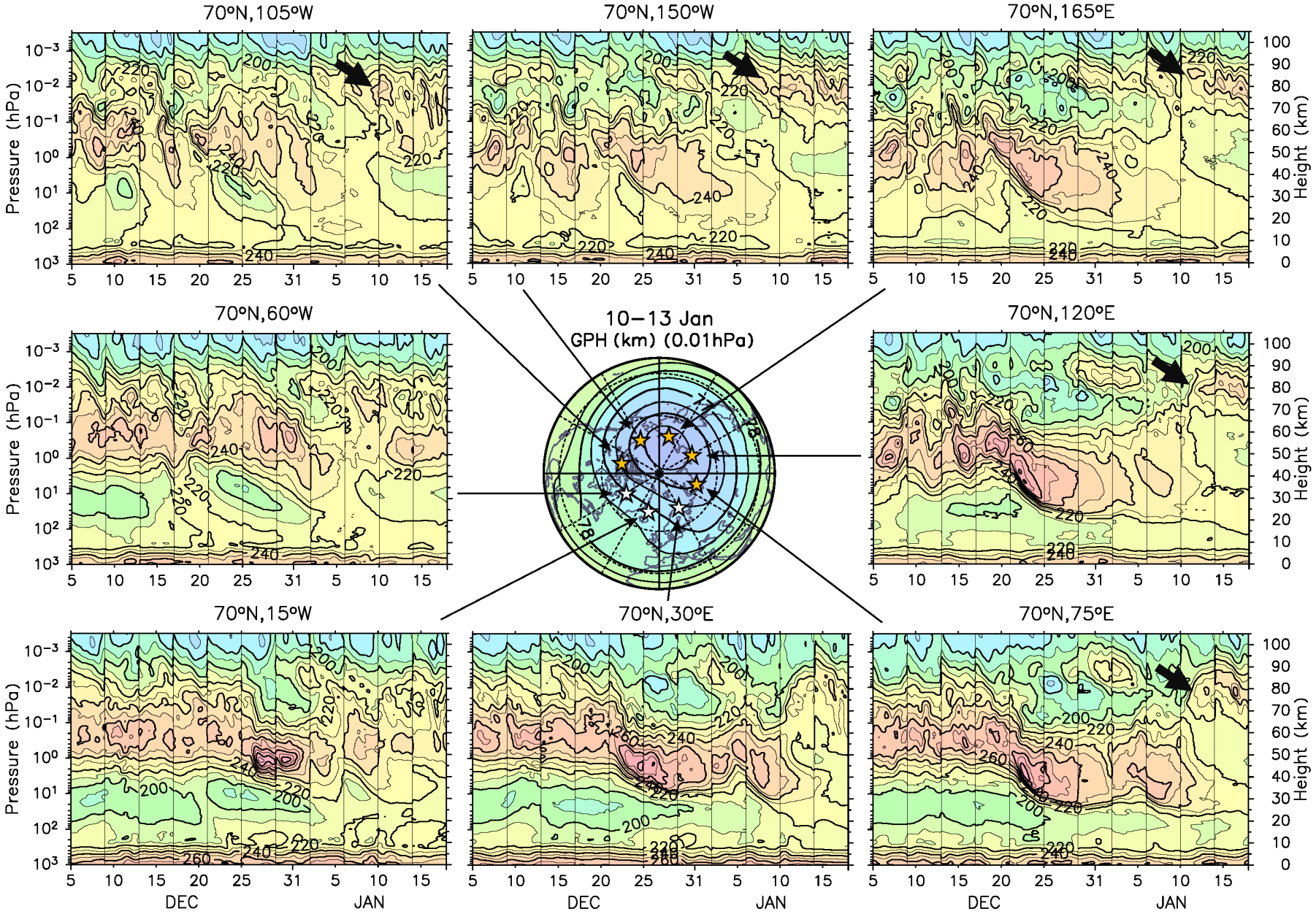

Map of GPH (unit: km) at 0.01hPa from 10-13 Jan. and time-height sections of T at each location along 70°N. The colors of stars represent the DS occurrence (yellow→the DS occurs).

Longitudinal structure of the ES

The ES is observed in the east of 150°E to 20°W.

In the region with $\bar{u}$<0 at z=25-40km, upward propagation of PW is barely observed. Most PWs from the troposphere cannot reach above z=80km.

The distribution of GWF<0 above z=75km is consistent with the ES structure.

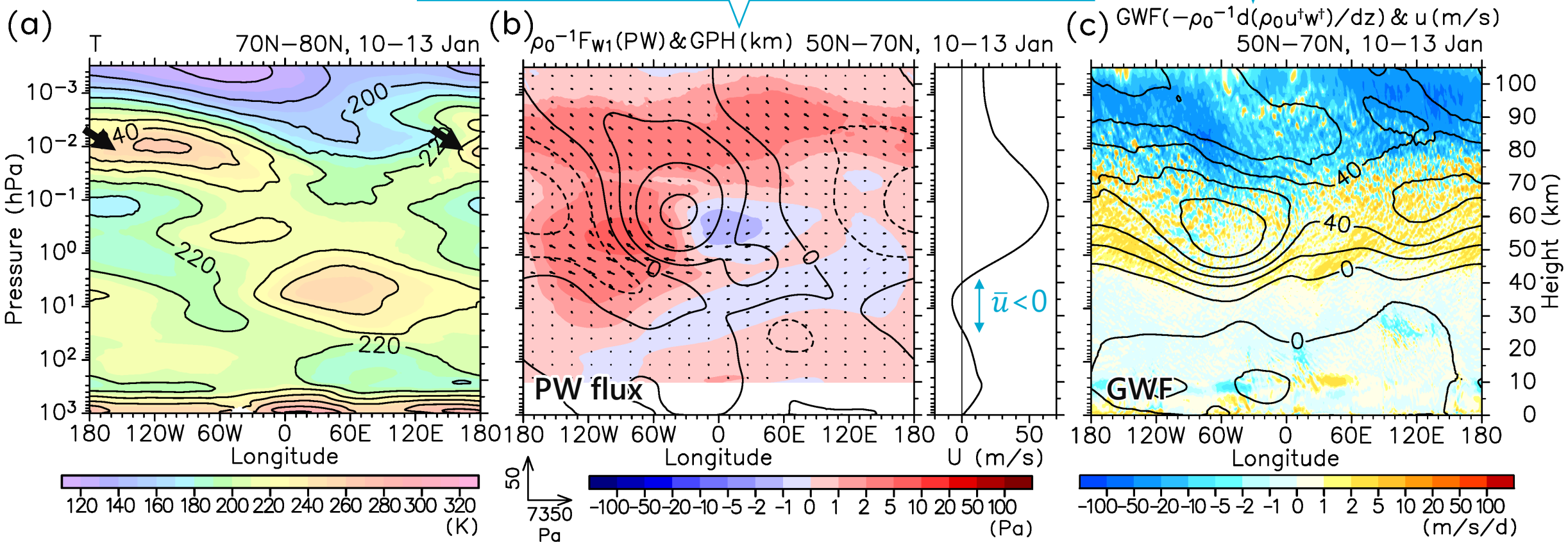

Longitude-height sections for 10-13 Jan. of (a) 50°N-70°N mean T, (b) 50°N-70°N mean 3D wave activity flux F_{W1} [Kinoshita & Sato 2013; Sato et al. 2013] (color represents the vertical component of F_{W1}) and geopotential height deviation from the zonal mean (contours; interval: 0.5km), and (c) GWF indicated by $-\rho_0^{-1}d(\rho_0 u'w')/dz$ and zonal wind u (contours; interval: 10m/s). A small box in (b) shows $\bar{u}$ profile.

ES formation: PW generation due to PWF

Where are PWs at z>80km from, which contribute to the ES formation along with GWs?

(1) During 6-9 Jan., prevailing **PWF<0** through the entire winter polar middle atmosphere (z>30km) appears (◯in Fig.1c).

(2) MPV peak is formed at ~60N, θ=4000K due to redistribution of MPV & mixing due to PW breaking (◯in Fig.1b & Fig.2).

(3) The necessary condition for BT/BC instability ($\overline{\mathrm{MPV}}_y$<0) is fulfilled poleward of the peak.

(4) During 10-13 Jan., **PWF>0**, which indicates PW generation, is observed poleward of the MPV peak & negative $\overline{\mathrm{MPV}}_y$ becomes small (◌in Figs.1f & 1g)).

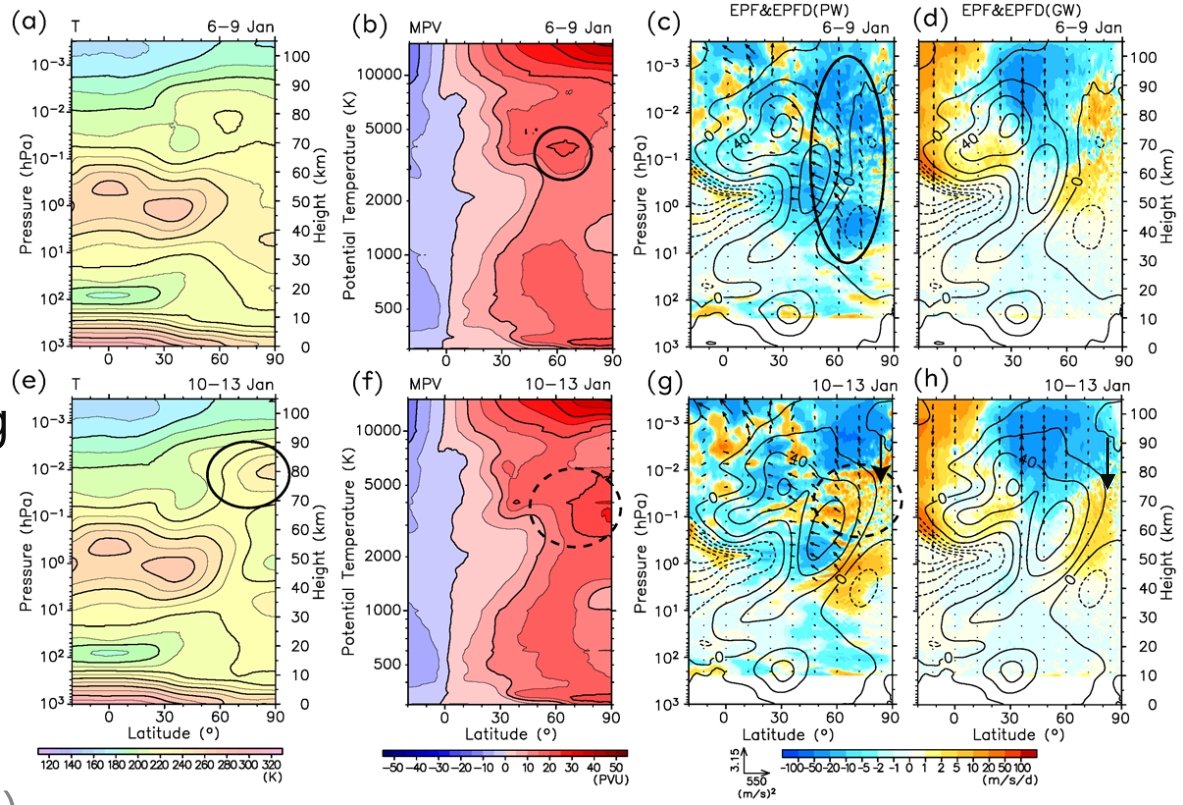

PWs are generated by the BT/BC instability which is induced by **PWF**.

GW-&PW-driven ES formation

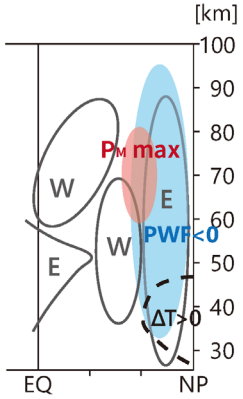

Figure 1(↗) Latitude-height sections of (a,e) $\overline{T}$, (b,f) $\overline{\mathrm{MPV}}$, (c,g) PWF and (d,h) GWF along with zonal wind u (contours; interval: 20m/s) for (a-d) 6-9 and (e-h) 10-13 Dec.

Figure 2(→) Maps at 0.05hPa for 6-9 Jan. of (a) MPV (color) and GPH (contour, unit:km) and (b) N^2

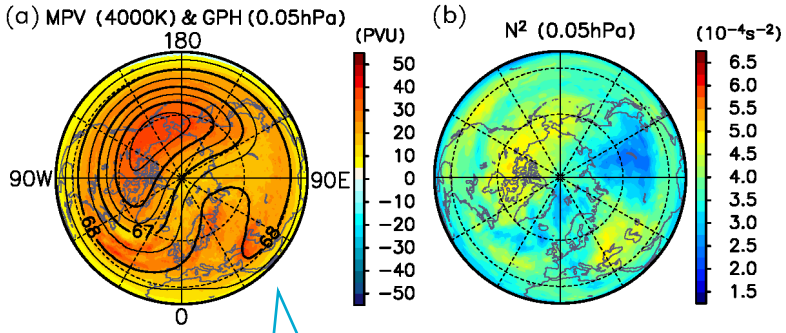

Comma-like vortex distortion: typical for PW breaking

Summary

To clarify the mechanisms of dynamical variation in the middle atmosphere during an SSW-ES event, a hindcast of the 2018/19 SSW event was carried out by a GW-permitting high-top GCM. The results were analyzed in terms of the interplay of PWs and GWs.

- During 2018/19 SSW, a temperature peak (topside of a mesospheric inversion layer) appeared at z=85-90km before the disappearance of the lowered stratopause.

  ⇒ Temperature structure with two peaks in the vertical: "double stratopause (DS)"
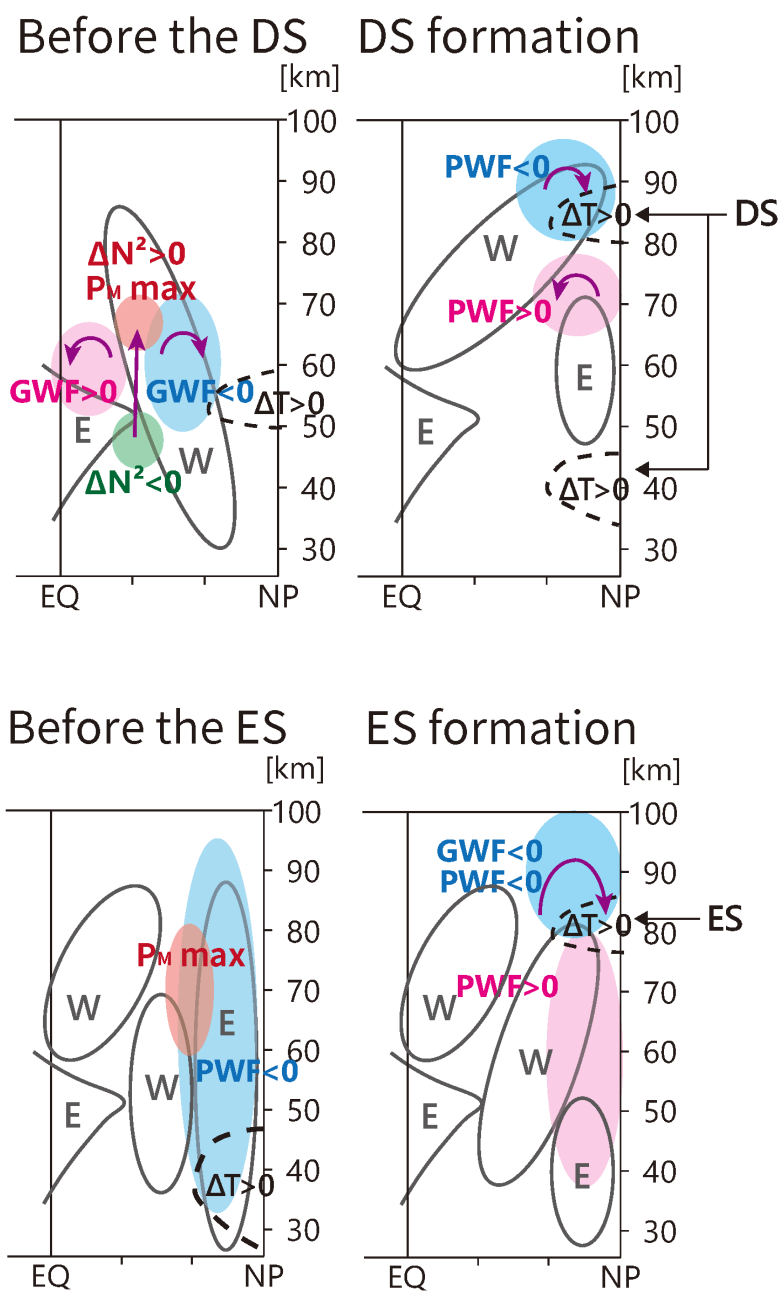
- The DS formation: PWF is **directly** responsible
- The ES (elevated stratopause) formation: Both PWF & GWF are responsible
- PWs that contribute to the DS (ES) formation are generated in the middle atmosphere through the BT/BC instability induced by GWF (PWF).